

Using Copolymers to Design Tunable Stimuli-Responsive Brushes

Shuanhu Qi,* Leonid I. Klushin, Alexander M. Skvortsov, and Friederike Schmid

Cite This: *Macromolecules* 2020, 53, 5326–5336

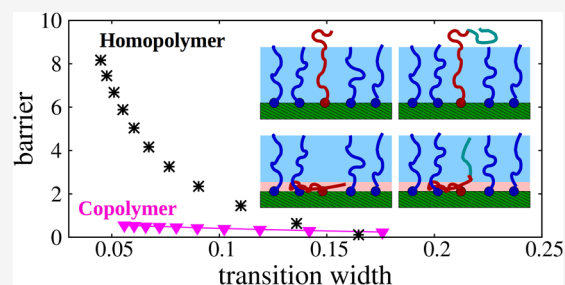
Read Online

ACCESS |

Metrics & More

Article Recommendations

ABSTRACT: Recently, a new design for switch sensors has been proposed that exploits a conformational transition of end-grafted minority adsorption-active homopolymers in a monodisperse polymer brush [Klushin et al. *Phys. Rev. Lett.* **2014**, *113*, 068303]. The transition is sharp and first-order type if the minority chain is longer than the brush chains. However, the intrinsic nature of the system imposes a constraint on the relation between the sharpness of the transition and the height of the free energy barrier controlling the transition kinetics: The sharper the transition, the slower the transition time. Here we demonstrate that adopting diblock copolymers with the adsorption-active block anchored at the substrate as the minority chains allows a much more flexible control of the three main characteristics of the transition, i.e., the transition point, its sharpness, and the barrier height. In particular, the barrier height can be greatly reduced without compromising the sharpness. We develop an analytical theory that predicts the relevant characteristics of the transition and verify it with SCF calculations and Monte Carlo simulations. We also demonstrate that from a thermodynamic point of view the transition characteristics of a diblock copolymer are equivalent to those of the active block alone in a modified brush with the same grafting density and reduced length.



INTRODUCTION

Stimuli-responsive polymers are smart materials in the sense that they are capable of conformational or chemical response to changes of specific external stimuli, such as environmental temperature, pH, light, and electric or magnetic fields.^{1–3} Because of the small dimensions and fast dynamics of the molecule structures, stimuli-responsive polymers can be exploited for the design of nanocargoes, switch sensors, which could find application in biomedicine or material engineering, e.g., for drug delivery or smart surfaces.^{4,5} In particular, multicomponent brushes have been recognized as interesting candidates for smart surfaces that can, for example, change their wettability in response to external stimuli.^{6,7} Experimental studies indicate that such transitions occur in a temperature interval of $\Delta T \approx 30$ K on time scales of minutes or longer.

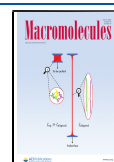
We have recently proposed a class of brush-based switches with much faster response times.^{8,9} The basic constituents are adsorption-responsive minority chains grafted on a substrate that is coated with a homopolymer brush. The minority chains are sufficiently dilute that the coupling between them is negligible. The interplay between the short-ranged adsorption to the substrate and the osmotic repulsion from the matrix brush chains induces a conformational transition in the minority chain between a desorbed (stretched) state, when the adsorption is weak, and an adsorbed state, when the adsorption is strong. The nature of the transition depends on the relative length of the minority chain. If the minority chain

is shorter than the brush chains (i.e., the degree of polymerization is smaller than that of the brush chains), the excluded volume repulsion imposed by the surrounding brush chains is screened. In that case, the minority chain behaves as an ideal chain, and the adsorption–desorption phase transition is continuous (second order), similar to the adsorption transition of a single grafted chain on the bare (attractive) substrate.^{10–12} If the minority chain is longer than the brush chains, it adopts an inhomogeneous flowerlike conformation in the desorbed state with a strongly stretched stem inside the brush and a randomly coiled crown outside the brush. The transition between this flowerlike state, where the chain end is preferable located outside of the brush, and the adsorbed state, where the chain is fully covered by the brush, is of first-order type and thus much sharper.^{13,14} The sharpness of the transition can be controlled by tuning the length of the minority chain. On the basis of this transition, one could design switch sensors that can trigger chemical reactions or immune response. For example, one could attach specific catalysts to the free end of the minority chain, such that a reaction in the solution outside of the brush can be initiated or

Received: March 23, 2020

Revised: May 18, 2020

Published: June 15, 2020



switched off by controlling the contact of the free end with the solution.^{15,16}

Because the switching transition involves conformational changes of single chains only and does not require cooperative rearrangements, it is expected to be fast. However, the switching time still depends on the height of the free energy barrier between the coexisting states. Unfortunately, the sharpness of the transition, which determines the sensitivity of the sensors, and the barrier height, which determines its response time, cannot be varied independently. Instead, one has a trade-off between the two, such that high sensitivity comes at the price of longer response times. The relation between the sharpness and barrier height seems largely independent of the structure of the underlying brush matrix.¹⁷ This seems to prohibit further improvement of the performance of switch sensors.

To overcome this problem, in the present work, we propose an alternative design where the switch chain is replaced by a grafted diblock copolymer. The idea is to decouple the two competing factors that drive the transition, i.e., the chain adsorption and the chain repulsion from the brush. In the proposed setup, switch chains consist of an end-grafted adsorption active block and an inert block of variable length. The sharpness of the transition is then mostly determined by the length of the adsorption active block, whereas the barrier height can be controlled by the length of the inert block. In particular, we will show that the barrier height can be reduced to almost zero if the length of the inert block approaches that of the brush polymers. Hence, our new setup allows to design highly sensitive switches with ultrasmall response times. We study the system by a combination of a theoretical analysis, one-dimensional self-consistent field (SCF) calculations, and Monte Carlo (MC) simulations.

THEORETICAL CONSIDERATIONS

We start with a theoretical analysis of the problem. We consider a single diblock copolymer with an adsorption active block of length N_A and an inert of length N_I . The outer end of the A-block is attached to a substrate, which is furthermore covered by a monodisperse brush of polymers with length N_{br} at a grafting density σ . Polymers are modeled as Gaussian chains with purely repulsive monomer interactions characterized by an interaction parameter $\nu > 0$ (good solvent conditions). Hence, the nonbonded interaction energy has the form $H_I = \frac{\nu}{2} \int d\mathbf{r} \rho(\mathbf{r})$, where $\rho(\mathbf{r})$ is the local monomer density. In addition, adsorbed A-segments gain an energy $(-\epsilon)$.

We neglect the effect of the embedded adsorption-active chain on the surrounding brush. The chain thus experiences the repulsive mean-field potential of a pure homopolymer brush, which we will denote $V(z)$, in addition to the short-range attraction to the surface. The brush potential is approximated by the corresponding mean-field expression for laterally homogeneous polymer brushes in the strong stretching limit,¹⁸ i.e., the parabolic potential

$$V(z) = \nu \rho_{br}(z) = V_0 \left(1 - \frac{z^2}{H^2} \right) \quad (z \leq H) \quad (1)$$

($V(z) = 0$ otherwise), where z is the normal distance from the substrate, $V_0 = \frac{3}{2} \left(\frac{\pi \nu \sigma}{2} \right)^{2/3}$ is the potential at the surface

expressed in $k_B T$ units, and $H = N_{br} \left(\frac{4\sigma\nu}{\pi^2} \right)^{1/3}$ is the brush thickness expressed in segment length units, a .

Homopolymer Adsorption. The simplest case of an adsorption-active homopolymer of length N_A in a monodisperse brush formed by chains of length $N_{br} < N_A$ makes a good starting point for the theoretical analysis. We concentrate on three characteristics of the adsorption transition: the transition point, the barrier height at the transition, and the sharpness of the transition as affected by finite-chain length effects.

We start with a fully adsorbed chain conformation. Its partition function can be reduced to that of a chain interacting with the bare attractive substrate, with a correction for the effect of the mean-field brush potential $V(z)$. In the parameter range of interest, the relevant adsorption regime is sufficiently far from the critical point of adsorption that the adsorption blob comprises at most a few monomers. Under these conditions, the adsorbed chain is confined within a region $z \ll H$, so that $V(z) \simeq V_0$, and the partition function has the form

$$Q_{ads}(N_A) = e^{N_A(-V_0 + \mu(\epsilon))} \quad (2)$$

where the reference state with zero free energy is an ideal coil away from the brush and $-\mu(\epsilon)$ is the model-dependent adsorption free energy per monomer evaluated for the chain adsorbing on the bare substrate. It is assumed that the adsorbing chain is long enough so that $N_A \mu \gg 1$ and nonexponential prefactors can be dropped.

Next, we consider a typical out-of-equilibrium conformation consisting of an adsorbed part comprising $N_A - n$ monomers and a desorbed tail of length n , which is affected by the brush density profile but has no contacts with the substrate. The partition function factorizes (again up to a nonexponential prefactor) into a product of two terms

$$Q(n, N_A) = Q_{ads}(N_A - n) Q_{tail}(n) \quad (3)$$

The adsorbed part is still assumed to be large compared to one adsorption blob so that $Q_{ads}(N_A - n)$ can be calculated according to eq 2. The partition function of the tail, $Q_{tail}(n)$, is obtained from Green's function $G(z_0, z, n)$ which is a solution of the Edwards equation

$$\frac{\partial G(z_0, z, n)}{\partial n} = \frac{1}{6} \frac{\partial^2 G(z_0, z, n)}{\partial z^2} - V(z)G(z_0, z, n) + \delta(n)\delta(z - z_0) \quad (4)$$

where n is the number of monomers, $z_0 = 0$ since the tail originates at the surface, and z is the free end position. The potential includes only the brush-generated repulsive field, $V(z)$, but not the short-range attraction to the substrate since the tail by definition avoids any contacts with the substrate. The solution of the Edwards equation with the repulsive parabolic field was obtained in ref 13 and is in our case expressed as

$$G_{tail}(0, z, n) = \frac{\pi}{2} \left[\frac{3}{N_{br} \sin\left(\frac{\pi n}{2N_{br}}\right)} \right]^{3/2} z \times e^{-V_0 n - (3\pi/4N_{br}) \cot(\pi n/2N_{br}) z^2} \quad (5)$$

Modifications of this expression due to the finite parabolic potential range, $0 \leq z \leq H$, are particularly important when $n \geq N_{\text{br}}$ and were discussed in detail in ref 8. Our main interest here is the integrated partition function, $Q_{\text{tail}}(n) = \int dz G(0, z, n)$. It turns out that up to nonexponential prefactors the tail partition function has a simple form with two matching branches:

$$Q_{\text{tail}}(n) = \begin{cases} e^{-V_0 n}, & n \leq N_{\text{br}} \\ e^{-V_0 N_{\text{br}}}, & n > N_{\text{br}} \end{cases} \quad (6)$$

The first branch can be rationalized as the partition function of a weakly deformed coil with the size $R_n \sim n^{1/2} \ll H$, which therefore probes the brush potential $V(z) \simeq V_0$. The fact that this result is quite accurate up to $n = N_{\text{br}}$ is a special property of the parabolic potential. The second branch describes the inhomogeneous flower conformation of the sufficiently long tail with $n > N_{\text{br}}$ ¹³ where the only nontrivial contribution comes from the stem of length N_{br} while the crown comprising the last $(n - N_{\text{br}})$ monomers form a coil outside the brush corresponding to the reference state.

Combining all the results above, we can now calculate the nonequilibrium free energy of a partially adsorbed state, $F(n; N_A) = -\log Q(n, N_A)$. Within the approximations introduced above, i.e., using eqs 2, 3, and 6, we obtain the simple piecewise linear function

$$F(n) = \begin{cases} F_{\text{ads}} + n\mu, & n \leq N_{\text{br}} \\ F_{\text{ads}} + V_0 N_{\text{br}} + n(\mu - V_0), & n > N_{\text{br}} \end{cases} \quad (7)$$

Here we have introduced the shortcut notation F_{ads} for the equilibrium free energy of the fully adsorbed chain.

The curves for the nonequilibrium free energy $F(n)$ representing different scenarios are sketched in Figure 1

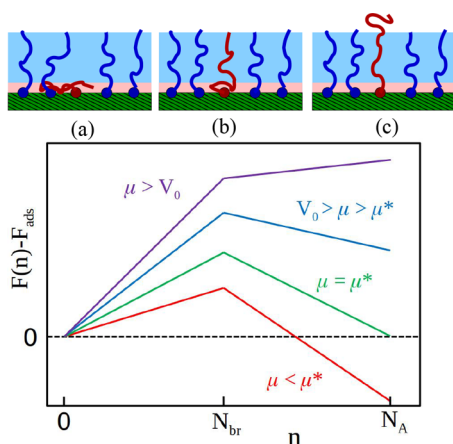


Figure 1. Top: cartoons showing the conformations of a homopolymer switch chain in the adsorbed state (a), the transition state (free energy maximum) (b), and the desorbed state (c). Brush chains are drawn in blue and minority chain in red. The light red region indicates the adsorption region. Bottom: sketch of the corresponding nonequilibrium free energy as a function of the length n of the desorbed tail for different values of the adsorption chemical potential, μ . The equilibrium state corresponds to the state with the deepest minimum. Different scenarios are shown for different adsorption strengths decreasing from top to bottom; see the discussion in the text.

together with cartoons showing the chain conformations in the adsorbed state ($n = 0$), in the transition state ($n = N_{\text{br}}$), and in the desorbed state ($n = N_A$). It is clear that if the adsorption is too strong, i.e., $\mu > V_0$, $F(n)$ is a monotonically increasing function, all the partially torn-off states with any n are absolutely unstable, and there can be no desorbed state at all, irrespective of N_A . In contrast, if $0 < \mu < V_0$, $F(n)$ is nonmonotonic: It initially increases linearly with a slope of μ but decreases for $n \geq N_{\text{br}}$. It has two local minima at the boundaries $n = 0$ and $n = N_A$: The first corresponds to the pure adsorbed phase, and the second corresponds to a completely desorbed state with the free energy

$$F_{\text{des}} = F(N_A) = V_0 N_{\text{br}} \quad (8)$$

The transition point is found from the condition $F_{\text{ads}} = F_{\text{des}}$, which gives

$$\mu^* = V_0 \frac{\Delta}{N_A} \quad (9)$$

where $\Delta = N_A - N_{\text{br}}$ is the excess length of the adsorption-active chain. The transition barrier emerges naturally from the nonmonotonic behavior of $F(n)$: The point $n = N_{\text{br}}$ defines the position of the barrier while its height with respect to the fully adsorbed state is given by μN_{br} . At the transition point, one obtains the barrier height

$$U_{\text{barrier}} = V_0 \frac{\Delta}{N_A} N_{\text{br}} \simeq \begin{cases} V_0 \Delta, & \Delta \ll N_{\text{br}} \\ V_0 N_{\text{br}}, & \Delta \gg N_{\text{br}} \end{cases} \quad (10)$$

In our earlier discussion^{8,9} we were concerned only with the case $\Delta \ll N_{\text{br}}$ and used a simplified expression for the barrier height, $U_{\text{barrier}} \simeq V_0 \Delta$. At fixed N_{br} the barrier height increases monotonically with the length of the adsorption-active chain, N_A , saturating at the limiting value of $V_0 N_{\text{br}}$. The general expression of eq 10 is valid for arbitrary $N_A > N_{\text{br}}$. The barrier height scaled by the factor $V_0 N_A$ turns out to be a universal quadratic function of the ratio N_{br}/N_A :

$$\frac{U_{\text{barrier}}}{V_0 N_A} = \frac{N_{\text{br}}}{N_A} \left(1 - \frac{N_{\text{br}}}{N_A} \right) \quad (11)$$

The barrier height vanishes in the limit of $N_{\text{br}} \rightarrow 0$ when the brush disappears and also in the limit of $N_{\text{br}} \rightarrow N_A$ when the excess length of the adsorption-active chain vanishes and the adsorption transition becomes continuous. Remarkably, the scaled barrier height is a symmetric function on the interval $0 < N_{\text{br}}/N_A < 1$ with a maximum at $N_{\text{br}}/N_A = 1/2$.

To discuss the shift in the critical point, one has to invert the function $\mu(\epsilon)$. It is known for ideal chains that close to the critical adsorption point (ϵ_c) this function is quadratic in $\epsilon_c - \epsilon$ while for strong adsorption $\mu \simeq -\epsilon$.^{35–37} This behavior is not affected much by excluded volume interactions. In general, the transition point must be described by a function of a single combination of parameters related to the brush and the adsorption-active chain:

$$-\epsilon^* = \psi \left(V_0 \frac{\Delta}{N_A} \right) \quad (12)$$

where ψ is the inverse of the function $\mu(-\epsilon)$ which generally depends on the specifics of the adsorption potential and interpolates between $\psi(x) + \epsilon_c \propto x^{1/2}$ at small values of the argument x and $\psi(x) \sim x$ at large x .

The transition width can be related to the slope of the adsorption curve with respect to ε at the transition point ε^* . To estimate it, we take the average height of the free end as the observable indicator of the transition and adopt a two-state model. In the desorbed state, we take $Z_c \simeq H$, where H is the brush height, and assume that the statistical weight $e^{-F_{\text{des}}}$ is independent of ε . In the adsorbed state, we approximate $Z_c \simeq 0$ and simplify the expression for the statistical weight by linearizing the exponent near the transition point, $e^{-F_{\text{ads}}(\varepsilon)} \approx e^{-F_{\text{ads}} - N_A \theta^* (\varepsilon - \varepsilon^*)}$, where $\theta^* = -\frac{d\mu}{d\varepsilon}|_{\varepsilon=\varepsilon^*}$ is the fraction of adsorbed monomers in the adsorbed subphase at the transition. Defining the transition width as $\delta\varepsilon = \left[\frac{1}{H} \frac{dZ_c}{d\varepsilon} \Big|_{\varepsilon=\varepsilon^*} \right]^{-1}$ the two-state model³⁸ gives

$$\delta\varepsilon = 4(N_A \theta^*)^{-1} \quad (13)$$

As discussed in the Introduction, the transition sharpness and the barrier height are two important parameters that control the sensitivity and the response time of the transition. A sharp transition with a low barrier is desirable from the application point of view. Combining eqs 10 and 13, one can relate these two characteristics to one another:

$$U_{\text{barrier}} = V_0 N_{\text{br}} - \frac{1}{4} V_0 N_{\text{br}}^2 \theta^* \delta\varepsilon \quad (14)$$

Diblock Copolymer Adsorption. Next we consider block copolymers. The theoretical analysis follows closely the derivation of eqs 2–14 with a few modifications: The free energy of the inert block must be accounted for in the adsorbed state:

$$F_{\text{ads}} = (V_0 - \mu)N_A + V_0(N_{\text{br}} - \tilde{N}_{\text{br}}) \quad (15)$$

where we have defined the effective brush length

$$\tilde{N}_{\text{br}} := \begin{cases} N_{\text{br}} - N_I, & N_I < N_{\text{br}} \\ 0, & N_I > N_{\text{br}} \end{cases} \quad (16)$$

With the redefined F_{ads} , we rewrite the free energy $F(n)$ as

$$F(n) = \begin{cases} F_{\text{ads}} + \mu n, & n \leq \tilde{N}_{\text{br}} \\ F_{\text{ads}} + V_0 \tilde{N}_{\text{br}} + (\mu - V_0)n, & n \geq \tilde{N}_{\text{br}} \end{cases} \quad (17)$$

Both the increasing and the decreasing linear branches of the $F(n)$ function retain their shape, but the crossover point where they match changes. For $N_I < N_{\text{br}}$, $F(n)$ switches from one branch to the other once the length of the desorbed subphase matches the effective brush chain length (\tilde{N}_{br}) (see cartoons in Figure 2). For $N_I > N_{\text{br}}$, i.e., $\tilde{N}_{\text{br}} = 0$, the curve for $F(n)$ directly enters the second branch.

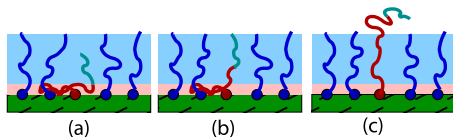


Figure 2. Cartoons showing the conformations of a copolymer switch chain in the adsorbed state (a), the transition state (free energy maximum) (b), and the desorbed state (c). Brush chains are drawn in blue. The light red region indicates the adsorption region. The active block in the minority chain is marked in red, and the inert block is marked in green. Monomers in the inert block and brush monomers have the same chemical properties.

Now the tail consists of n monomers of the adsorption-active block and N_I monomers of the inert block; hence, the position of the barrier top is given by $n^* = \tilde{N}_{\text{br}}$. The free energy of the fully desorbed chain is still described by eq 8 without any changes.

Provided $N_A > \tilde{N}_{\text{br}}$, the transition point ε^* is determined by $-\varepsilon^* = \psi(\mu^*)$ with the modified adsorption chemical potential

$$\mu^* = V_0 \left(1 - \frac{\tilde{N}_{\text{br}}}{N_A} \right) =: V_0 \frac{\Delta}{N_A} \quad (18)$$

Equation 18 defines the coexistence line separating the adsorbed and desorbed states in the phase diagram for adsorption active diblock copolymers in a monodisperse brush. The phase diagram for the homopolymer limit, $N_I = 0$, was discussed earlier in ref 14. Here the effective excess length of the diblock copolymer can be written in two equivalent forms

$$\Delta = N_A - \tilde{N}_{\text{br}} = \begin{cases} N_A + N_I - N_{\text{br}}, & N_I < N_{\text{br}} \\ N_A, & N_I \geq N_{\text{br}} \end{cases} \quad (19)$$

The barrier height at the transition is given by

$$U_{\text{barrier}} = \mu^* n^* = V_0 \tilde{N}_{\text{br}} \frac{\Delta}{N_A} = V_0 \tilde{N}_{\text{br}} \frac{N_A - \tilde{N}_{\text{br}}}{N_A} \quad (20)$$

When scaled by $V_0 N_A$, it becomes a universal parabolic function of the ratio $\tilde{N}_{\text{br}}/N_A$:

$$\frac{U_{\text{barrier}}}{V_0 N_A} = \frac{\tilde{N}_{\text{br}}}{N_A} \left(1 - \frac{\tilde{N}_{\text{br}}}{N_A} \right) \quad (21)$$

The scaling relation for the transition sharpness

$$\delta\varepsilon = 4(N_A \theta^*)^{-1} \quad (22)$$

is the same as that for homopolymers (eq 13). The connection between the barrier height and the transition width is given by

$$U_{\text{barrier}} = V_0 \tilde{N}_{\text{br}} - \frac{1}{4} V_0 \tilde{N}_{\text{br}}^2 \theta^* \delta\varepsilon \quad (23)$$

Hence, U_{barrier} is now decoupled from the transition width, $\delta\varepsilon$. Whereas $\delta\varepsilon$ depends on the length of the active block only N_A , the barrier height U_{barrier} can additionally be tuned by varying \tilde{N}_{br} via a manipulation of the inert block length, N_I .

Comparing eqs 9 and 10 to eqs 18 and 20, one notices that the results for the homopolymer and the diblock cases become identical if one replaces the brush chain length, N_{br} , in the homopolymer equations by the effective brush length, \tilde{N}_{br} , to account for the effect of the inert block.

NUMERICAL CALCULATIONS

To test the ideas developed in the previous section, we study the system described above by numerical SCF studies and MC simulations.

Model System. Specifically, our model system is composed of a monodisperse brush and a diblock copolymer as the minority chain in a volume $V = L_x L_y L_z$. We set periodic boundaries along the x and y directions, while impenetrable walls are placed at $z = 0$ and $z = L_z$. All chains are grafted with one end each chain to a “substrate” located at $z = z_0$, where z_0 is chosen smaller than the statistical bond length rather than zero for practical reasons. Polymer chains are modeled as monomers (beads) connected by Gaussian springs with spring constant $3k_B T/a^2$, where a is the statistical bond length and

$k_B T$ the thermal energy. Hereafter, we will use $a \equiv 1$ as the length unit and $k_B T \equiv 1$ as the energy unit. The total number of monomers in a brush chain (referred as the length of the chain) is denoted as N_{br} , while that in the minority chain is written as $N = N_A + N_I$, where N_A and N_I are the length of the active block and the inert block, respectively. In the vicinity of the impenetrable wall at $z = 0$, active monomers in the minority chain experience an additional attractive potential $U_{ads}(z)$, which is a steplike function with magnitude $(-\varepsilon)$ covering a range $0 \leq z \leq a$ (with $\varepsilon > 0$).

The total energy in the system includes three contributions: the bonded interaction H_0 , the nonbonded monomer–monomer interaction H_I , and the active monomer adsorption energy H_{ads} . The bonded interaction arises from the spring elasticity and is given by $H_0 = \frac{3}{2} \sum_{\alpha j} (\mathbf{R}_{\alpha j} - \mathbf{R}_{\alpha, j-1})^2$, where α labels chains and j labels monomers. The nonbonded interaction comes from the excluded volume repulsion and is written as a function of local density, i.e., $H_I = \frac{\nu}{2} \int d\mathbf{r} \hat{\rho}_t^2(\mathbf{r})$, where $\hat{\rho}_t(\mathbf{r}) \equiv \sum_{\alpha j} \delta(\mathbf{r} - \mathbf{R}_{\alpha j})$ is the microscopic monomer density, and the sum runs over all monomers.^{19,20} The adsorption energy is expressed as $H_{ads} = \sum_j U_{ads}(z)$, where j runs over all N_A active monomers in the minority chain.

This system is studied mainly by SCF theory. For comparison, we also run MC simulations for some selected minority chain lengths. Details of the numerical methods are given in the Appendix. The model parameters are $N_{br} = 100$, $\sigma = 0.1$ (the grafting density), and $\nu = 0.776$ in the SCF calculations and $\nu = 1$ in the MC simulations. The excluded volume parameter ν in the SCF calculations has been renormalized, compared to the MC model, to account for fluctuation and discretization effects (see the Appendix and ref 9). For comparison, SCF calculations were also performed for higher grafting densities up to $\sigma = 0.3$ (data not shown). The results are qualitatively the same.

To characterize the transition, we evaluate the free end distribution P_e , i.e., the probability to find the N th monomer at position z (see the Appendix), and the average height of the free end, $Z_e = \int dz z P_e(z)$. From these two we extract the transition point $-\varepsilon^*$, the transition width $\delta\varepsilon$, and the free energy barrier $U_{barrier}$ separating the adsorbed and the desorbed states.

The transition width (i.e., the inverse transition sharpness) is defined from the profile of Z_e as follows: First, one finds the maximum slope of the profile, and then one evaluates the transition width through

$$\delta\varepsilon = \left| \frac{Z_e(\varepsilon = 0) - Z_e(\varepsilon = -\infty)}{\left. \frac{dZ_e}{d\varepsilon} \right|_{\max}} \right| \quad (24)$$

The transition width is a measure of the change of the adsorption energy during the transition. At small $\delta\varepsilon$, the transition takes place in a narrow window of ε , thus $\delta\varepsilon$ characterizes the sensitivity of the transition. At the transition point, the adsorbed state and the desorbed state coexist; therefore, the distribution P_e has a bimodal structure, and we define the transition point as the specific adsorption strength $(-\varepsilon^*)$ where the two maxima in the profile P_e have equal height. In addition, the transition barrier $U_{barrier}$ is extracted from the distribution P_e by calculating the effective potential,

$U_{eff}(z) = -\ln P_e(z)$, at the transition point and then determining the energy barrier between the two minima of $U_{eff}(z)$. As discussed earlier, the transition barrier determines the transition time τ_e . If the barrier in units of $k_B T$ is much larger than unity, the dominant dependence is exponential,³⁴ i.e., $\tau_e \propto e^{U_{barrier}}$.

Results of the SCF Calculations. We focus on block copolymers with total chain length $N > N_{br}$ and inert block length $0 < N_I < N_{br}$, which is the most relevant regime according to the theoretical analysis in the previous section. At $N < N_{br}$, the adsorption transition is smooth and uninteresting in the context of switch design. For $N_I > N_{br}$, the effective brush length remains constant, $\tilde{N}_{br} = 0$ according to eq 16, and the characteristics of the transition should be the same as for $N_I = N_{br}$.

Before investigating the switch transition in detail, we test the theoretical prediction that the behavior of diblock copolymers at the transition should correspond to that of homopolymers in a shorter brush with effective brush length $\tilde{N}_{br} = N_{br} - N_I$. This equivalence is not obvious. We illustrate it in Figure 3 for different copolymer test cases. Specifically, we

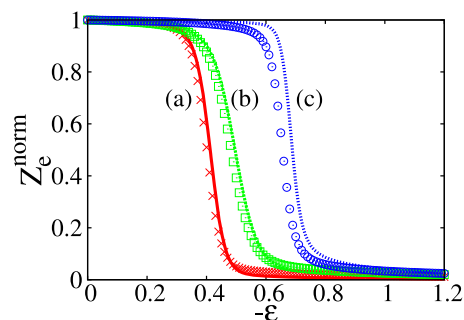


Figure 3. Comparison of the normalized adsorption curves for diblock chains in a brush with $N_{br} = 100$ (lines) and an equivalent homopolymer with the same N_A in an effective brush with $\tilde{N}_{br} = N_{br} - N_I$ (symbols): (a) diblock copolymer parameters $N_A = 75$, $N_I = 50$ and homopolymer parameters $N_A = 75$, $\tilde{N}_{br} = 50$; (b) diblock copolymer parameters $N_A = 50$, $N_I = 75$ and homopolymer parameters $N_A = 50$, $\tilde{N}_{br} = 25$; (c) diblock copolymer parameters $N_A = 100$, $N_I = 90$ and homopolymer parameters $N_A = 100$, $\tilde{N}_{br} = 10$. The brush grafting density is the same everywhere $\sigma = 0.1$. The average end height Z_e^{norm} is normalized such that it varies in the range between 0 in the adsorbed state and 1 in the fully desorbed state.

compare the adsorption curves of the copolymers and their equivalent homopolymer by plotting the normalized average free end height, $Z_e(\varepsilon)$, as a function of the adsorption energy, ε . Overall, the copolymer and equivalent homopolymer curves are very close to each other. Discrepancies are observed when the length of the equivalent brush is quite small, $\tilde{N}_{br} = 10$. The homopolymer curve is then shifted to the left (lower adsorption energies). We attribute this to the fact that details of the brush structure close to the brush edge become important for small \tilde{N}_{br} . Despite small shifts of the transition point, the shape of the adsorption curves (and hence the transition sharpness) is almost identical for the copolymer and the equivalent homopolymer.

Copolymers with Fixed Inert Block Length. We now turn to the discussion of the adsorption transition in systems with copolymers switch chains. We first consider the influence of the active block length, N_A , on the characteristics of the transition. We choose two fixed values of inert block length—

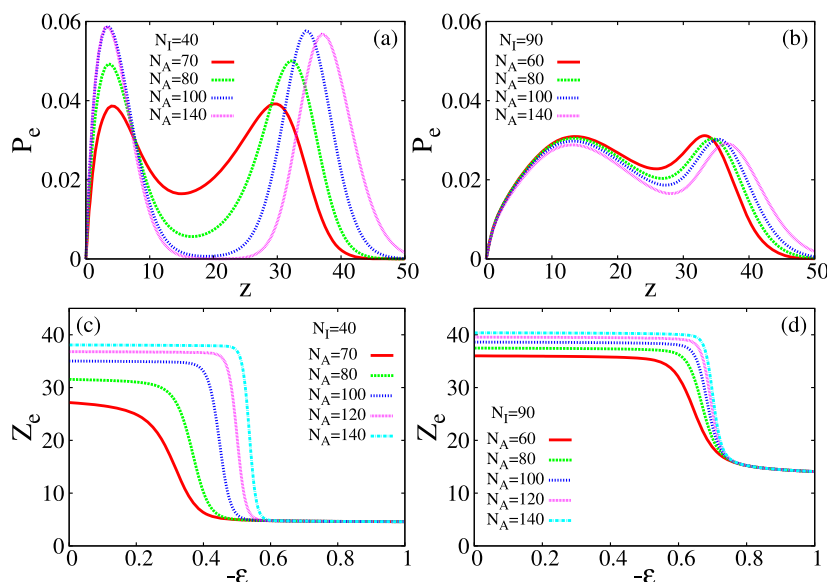


Figure 4. Free end distribution at the transition point for diblocks with short inert block $N_I = 40$ (a) and long inert block $N_I = 90$ (b) and adsorption curves for the average free end height $Z_e(\epsilon)$ for the case of short inert block (c) and long inert block (d). The brush length is $N_{br} = 100$, and the brush grafting density is $\sigma = 0.1$.

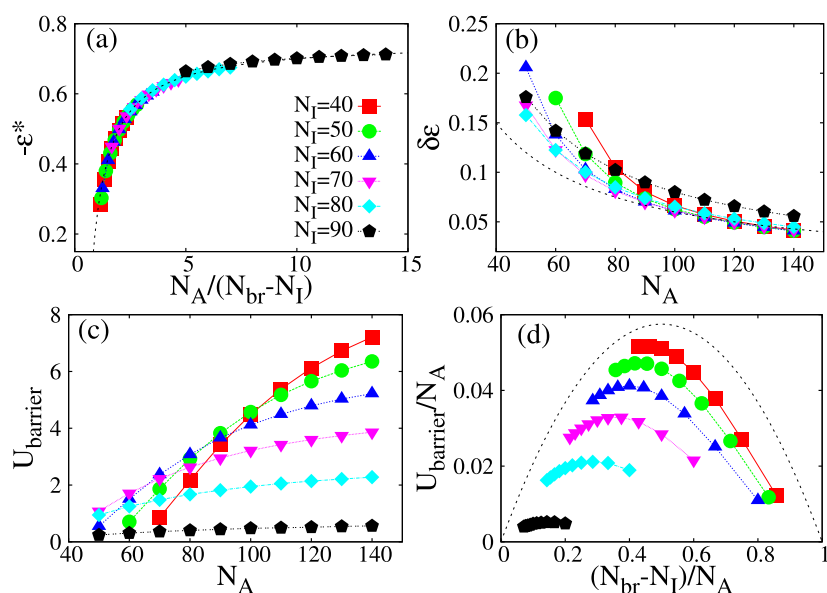


Figure 5. Transition point (a), transition width (b), transition barrier (c), and rescaled transition barrier (d) of the conformational transition of the free end as a function of N_A with several different N_I as indicated in (a) (the legend refers to all four panels). The grafting density of the brush is $\sigma = 0.1$. The solid line in (a) shows the function $0.25 + 0.5(1 - 1/x)$, the solid line in (b) the function $6/x$, and the solid line in (c) the function $0.23x(1 - x)$.

$N_I = 40$, noticeably smaller than $N_{br} = 100$, and $N_I = 90$, rather close to N_{br} —and vary N_A in a fairly broad range.

Figures 4a and 4b show the free end distribution measured at the transition point for a small and large inert block N_I , respectively, at different active block length. The bimodal structure clearly demonstrates the coexistence of the adsorbed state, represented by the maximum near the substrate, and the desorbed escape state, represented by the maximum located near the outer brush edge. The dip between the two maxima represents the barrier separating the two states at the transition. It generally becomes more pronounced with increasing N_A . However, in the case of a long inert block (with length close to the length of brush chains), the

distributions are almost flat, indicating that the barrier height is at most of order 1.

Figures 4c and 4d show Z_e as a function of the adsorption strength for short ($N_I = 40$) and long ($N_I = 90$) inert blocks and different N_A , respectively. The shape of these adsorption curves is characteristic of sharp first-order type transitions softened by finite-size effects (here: finite chain-length effects). In a well-defined state (adsorbed or desorbed), the chain conformation changes very little with ϵ , but near the transition point the drop in Z_e is quite dramatic. The transition point shifts systematically to larger adsorption strength with increasing active block length, N_A , although this shift is quite small when the inert block is long. Simultaneously, the

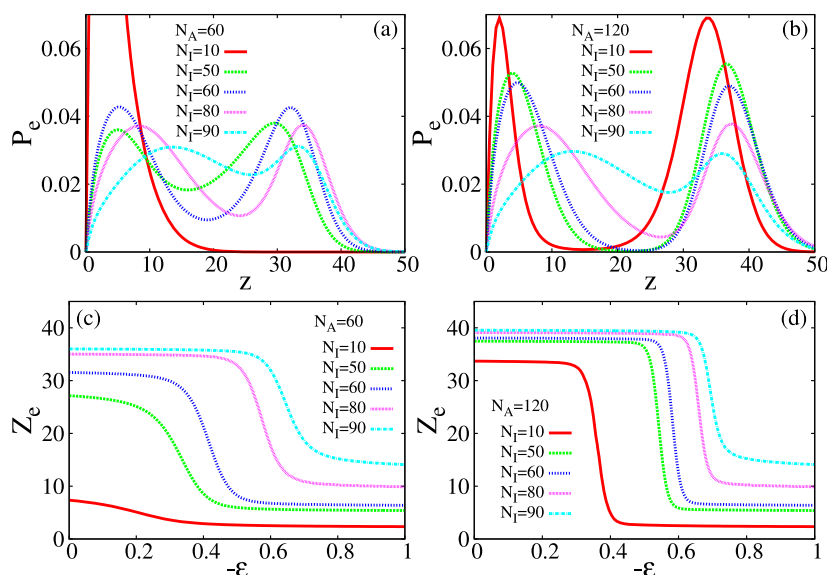


Figure 6. Free end distribution at the transition point for diblocks with short active block $N_A = 60$ (a) and long active block $N_A = 120$ (b) and the adsorption curves for the average free end height $Z_e(\epsilon)$ for the case of short active block (c) and long active block (d). The brush length is $N_{br} = 100$, and the brush grafting density is $\sigma = 0.1$.

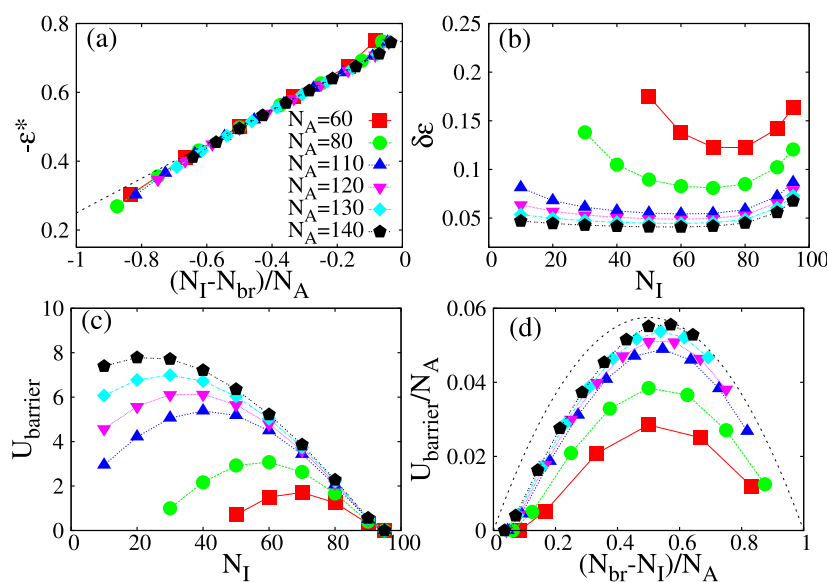


Figure 7. Transition point (a), transition width (b), transition barrier (c), and rescaled transition barrier (d) of the conformational transition of the free end as a function of N_I with several different N_A as indicated in (a) (the legend refers to all four panels). The brush length is $N_{br} = 100$, and the brush grafting density is $\sigma = 0.1$. The solid line in (a) shows the function $0.75 + 0.5x$, and the solid line in (c) shows the function $0.23x(1 - x)$.

sharpness of the transition also increases with N_A . In the case of the long inert block, the overall drop in Z_e is smaller because the free end position in the adsorbed state is farther away from the substrate. This is consistent with the expectation that the long inert block inside the brush is rather strongly deformed.¹³

Figure 5 summarizes the numerical data concerning the transition point, the transition width, and the transition barrier as a function of the length of the active block N_A for several inert block lengths N_I . The data for the transition point ϵ^* are plotted against the scaling variable $x = N_A/\tilde{N}_{br}$ suggested by the theory (eq 18). In agreement with the theoretical expectation, the data collapse onto a single master curve which first rises rapidly and then saturates. Assuming that the adsorption energy at the transition varies roughly linearly with the adsorption chemical potential (strong adsorption regime),

one obtains the relation $\epsilon^* = \epsilon_\infty^* - A/x$, which nicely fits the numerical data.

The transition width, $\delta\epsilon$, systematically decreases with increasing active block length N_A and is almost independent of N_I , especially for large N_A , in agreement with eq 22 (Figure 5b). Systematic deviations are only observed for $N_I = 90$, where the inert block length is close to the brush length. In that case, the approximate treatment of the brush as an Alexander brush may no longer be appropriate. The decay of $\delta\epsilon$ with N_A roughly follows the theoretical expectations, $\delta\epsilon \propto 1/N_A$. Finally, the barrier height $U_{barrier}$ increases with N_A , but the increase is reduced for larger inert block lengths N_I as expected (Figure 5c). If N_I approaches the length of brush chains, $U_{barrier}$ drops below one and becomes quasi-negligible. Figure 5d shows the same data rescaled in a way that the

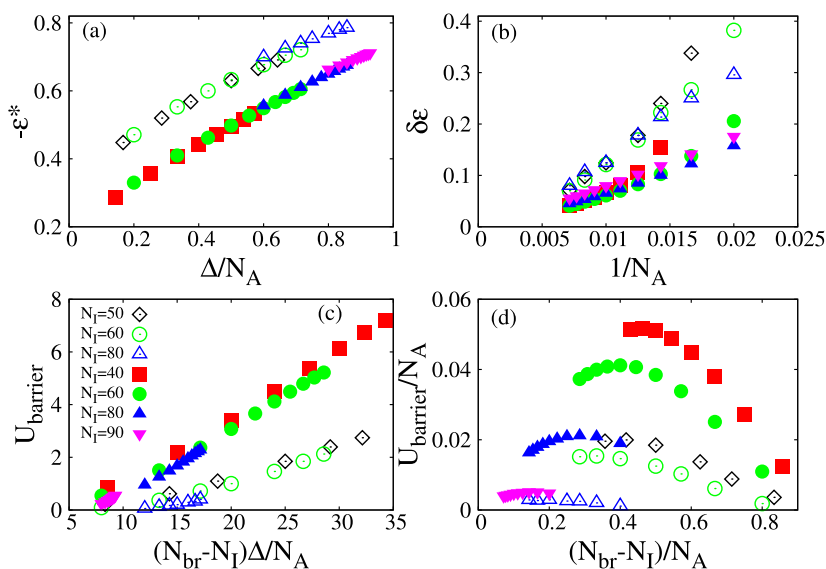


Figure 8. Comparison of transition point (a), transition width (b), and transition barrier (c, d) of the conformation transition as obtained from SCF calculations (filled symbols) and MC simulations (empty symbols) plotted as a function of the scaling variables suggested by the theory. The error of the MC data is comparable to the size of the symbols. The legend in (c) refers to all four panels. The length of the brush chains is $N_{br} = 100$, and the grafting density of the brush is $\sigma = 0.1$.

theory (eq 21) would predict a data collapse onto an inverse parabola. The collapse is not observed; however, the individual curves do reflect the predicted parabolic behavior. The analytical theory is based on the assumption that all the relevant changes in the free energies are large compared to $k_B T$. For a substantial portion of the SCF data sets the measured barrier heights are less than 3 or 4, and this is where the deviations from theory predictions are most noticeable.

Copolymers with Fixed Active Block Length. Next we study the influence of the inert block length on the transition in more detail. Figures 6a and 6b show the free end distributions measured at the transition point for a shorter ($N_A = 60$) and longer ($N_A = 120$) active block, respectively, at different active block lengths. The general shape is similar to what was described above. However, one can notice that the dip representing the free energy changes with the increase in N_I in a nonmonotonic way, first increasing and then decreasing.

Figures 6c and 6d show the adsorption curves for the average height of the free end $Z_e(\epsilon)$ in dependence of the adsorption energy for chains with short adsorption active block $N_A = 60$ and a longer active block $N_A = 120$ at several different inert block lengths. Increasing the inert block length shifts the transition point to larger adsorption strength but does not visibly affect the sharpness of the transition. As already mentioned above, the overall drop in Z_e at the transition region becomes noticeably smaller as the inert block length approaches the brush length.

Figure 7 presents the summary data for the transition point (a), the transition width (b), and the transition barrier (c) as a function of N_I with several different values of N_A . As already observed earlier and predicted from eq 18, the data for the transition adsorption energy ($-\epsilon^*$) collapse onto one curve if plotted against the single scaling parameter $x = (N_I - N_{br})/N_A$, and they increase roughly linearly with x . The transition width is a weakly nonmonotonic function of N_I and decreases with increasing N_A as noticed before. The dependence of the transition barrier on the length of the inert block N_I is also

nonmonotonic. If one increases N_I at fixed N_A , the potential barrier first increases and then decreases again. This behavior is in fact predicted by theory (eq 21). The barrier height is expected to vanish in two limiting cases: $N = N_I + N_A = N_{br}$ and $N_I = N_{br}$. In the first case, the minority chain has the same length than the brush chains, and the transition becomes second order. In the second case, the transition state (Figure 2b) coincides with the adsorbed state (Figure 2a): The transition is discontinuous but still barrier free.

Figure 7d shows the same data as Figure 7c but rescaled in the manner suggested by theory (eq 21). Data points for larger lengths of the adsorbing block N_A tend to collapse onto a single master curve, but cases with barriers lower than a few $k_B T$ fall outside the validity range of the theory with the strongest deviations corresponding to smallest barriers.

Comparison with MC Simulations. In the MC simulations, the height of the copolymer chain and its free end distribution can be measured directly. The transition point, transition width, and transition barrier are all extracted from those two quantities in a way the same as that adopted in the SCF method.

The results from the MC simulations are shown in Figure 8. The parameters are already rescaled as suggested by the theory. For example, theory (eq 18) predicts that the transition point ϵ^* should depend on the single parameter $\frac{\Delta}{N_A} V_0$. In our calculations, the grafting density is not varied; hence, the brush potential at the grafting plane, V_0 , is a constant. Therefore, we plot in Figure 8a the SCF and MC data for the transition adsorption energy, ϵ^* , as a function of $\frac{\Delta}{N_A}$. Indeed, all the SCF results fall nicely onto a single master curve (see also Figure 7b), and so do the results of the MC simulations. The master curves represent the coexistence lines in the phase diagram for the diblock adsorption, as mentioned in the discussion of eq 18. Compared to the SCF results, the MC data are shifted by a roughly constant offset, $\Delta\epsilon^* \sim 0.1$. This was already observed in our earlier homopolymer study⁹ and attributed to the fact that the chain behavior of chains in the MC model in close

vicinity of the surface is not captured properly by the SCF theory, since the attractive potential vanishes on the scale of the statistical bond length a .

Likewise, the MC data for the transition width, $\delta\varepsilon$, reproduce the $1/N_A$ scaling predicted by theory (eq 22), albeit with a different slope than that found in the SCF data (Figure 8b). Because the slope is given by $4/\theta^*$, we conclude that the SCF theory apparently overestimates the fraction θ^* of adsorbed monomers at the transition presumably due to chain discretization effects. Some data scattering at large values of $\delta\varepsilon$ can be traced back to the fact that the two-state model approximation used in the theory may lose its validity if the transition is smooth.

Finally, the SCF and MC data for the barrier height U_{barrier} also collapse onto single (but separate) master curves if plotted against the variable $(N_{\text{br}} - N_I) \frac{A}{N_A}$ and increase approximately linearly as a function of this parameter as predicted by theory (eq 20), albeit with a small offset of order one. The MC results are generally below the SCF results, and the slope of the curve is smaller. This was already observed for switches based on homopolymers⁹ and has been attributed to density fluctuations in real brushes close to the brush edge and to the corresponding fluctuations of minority configurations. As shown in Figure 10, the density profiles in the MC simulations are slightly steeper at the brush edge than those obtained by SCF calculations. As a result, the switch chain is less stretched in the exposed state, which reduces the potential barrier. Figure 8d shows the parabolic scaling plot of the barrier height. As in the previous SCF-based plots (Figures 5d and 7d), the data do not collapse, but they do demonstrate the parabolic behavior which can also be seen in the MC data.

SUMMARY AND CONCLUSION

The purpose of the present paper was to remove the shortcomings of a previously proposed design for brush-based switch surfaces with adsorption-active minority chains. In this design, the switching is triggered by a first-order conformational transition of a grafted minority chain. The transition width and the height of the transition barrier are central quantities that both need to be minimized to optimize the properties of the switch. In our previous, design, where the switch chain was a homopolymer, these quantities were strongly coupled to each other: if one was reduced, the other was increased. Another potentially weak point was that the switch could only operate close to the critical adsorption point. The aim of the present work was to overcome these limitations and allow a more flexible control of all the characteristics of the transition.

The basic idea of the new design is to attach one inert block to the free end of the adsorption-active homopolymer switch chain, turning it into a diblock copolymer. By increasing the adsorption strength, the diblock copolymer chain undergoes a first order conformational transition from exposed state to adsorbed state. Our study shows that in such a setup the transition width and the barrier height can be controlled independently by varying the length of the two blocks. Specifically, the transition can be made arbitrarily sharp by increasing the length of the adsorption active block, and the barrier height can practically be eliminated by increasing the length of the inert block. This is illustrated in Figure 9. From the point of view of designing sensitive switches with fast response times, diblock copolymers with a long adsorption-

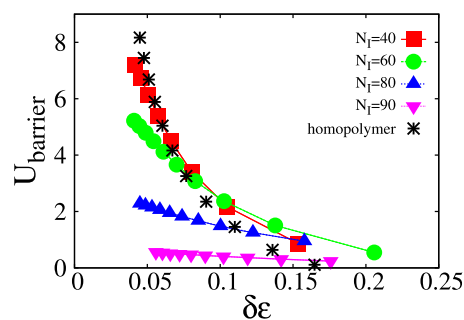


Figure 9. Transition barrier as a function of transition width for the transition of homopolymer chains (black asterisk) and diblock copolymer chains for fixed inert block lengths N_I as indicated and varying active block length N_A as obtained from SCF calculations. The brush length is $N_{\text{br}} = 100$, and the grafting density of the brush is $\sigma = 0.1$.

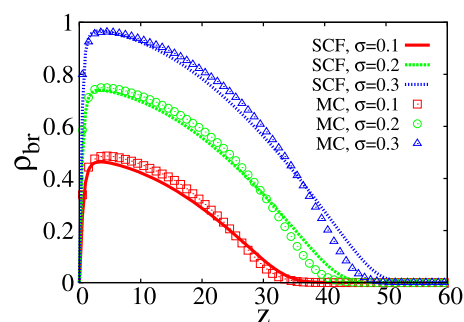


Figure 10. Density profiles of the monodisperse brush obtained by SCF theory (solid lines) and MC simulations (empty symbols). The excluded volume parameter in SCF method is set $\nu = 0.776$, while in MC simulations it is $\nu_{\text{MC}} = 1$. The brush height can be estimated as $H \approx 33$ for $\sigma = 0.1$, $H \approx 40$ for $\sigma = 0.2$, and $H \approx 50$ for $\sigma = 0.3$.

active block and an inert block with a length close to the brush chain length seem most promising.

An additional benefit of the new setup is that the length of the switch can be made arbitrary long by increasing the length N_A of the adsorption active block. This facilitates the design of switches that induce changes in the solution at some distance from the brush surface. For example, if such switches are used to turn on or off catalytic reactions, the use of longer switch polymers may increase the catalysis yield because they can extend farther into the solution and thus have larger probability to make contact with reaction agents.

We have validated our design by a combination of analytic theory, SCF calculations, and MC simulations. In general, the SCF and MC results are in good agreement with each other and confirm the scaling relations suggested by the theory. The comparison of SCF calculations and MC simulations provides insight into the possible effect of thermal fluctuations. Fluctuations tend to increase the transition width and decrease the transition barrier, but they do not modify the general picture.

For conventional first-order transitions, the switching time is dominated by the presence of a pronounced barrier according to the Arrhenius formula. When the barrier is of order $1 k_B T$ or even less, we expect the switching time be controlled by a faster, activation-free diffusion-type process.^{11,12}

In this study, we have taken the matrix brush to be monodisperse. In reality, brushes are polydisperse. However, the general idea which we put forward here—to use

copolymers to gain independent control over the sharpness of the transition and the transition barrier height—can also be applied if the brushes are polydisperse. Moreover, previous studies of homopolymer-based switches¹⁷ have shown, somewhat counterintuitively, that polydispersity tends to improve the quality and stability of the switches. Compared to a real situation, the present model is simplified. For example, the inert block is treated chemically the same as the brush chains, and this may not be the case in reality. In addition, the finite size of the end groups or attached specific receptors may also have an effect on the switching behavior, whereas the specific chemical structure of chain ends that are permanently located outside of the brush will not have a large influence on the free energy barrier for switching. On the other hand, for certain applications, it may be useful to attach functional groups at the side of the brush, close to the joint linking the active and inert block, such that they are exposed or buried depending on the state of the chain. The present work emphasizes the principal feature of block copolymer switches. However, to help real material design, more elaborated models should be developed, and this directs us to future studies.

■ APPENDIX

SCF Calculations

In the SCF theory, the model system with an Edwards type Hamiltonian is cast into a continuous description by the density field $\rho_t(\mathbf{r})$ and its conjugate potential $\omega(\mathbf{r})$.^{21,22} The total density $\rho_t \equiv \rho_{br} + \rho_m$ contains contributions from the polymer brush (ρ_{br}) and the minority chain (ρ_m). Local perturbations of the brush due to the presence of the minority chain are discarded. The single minority chain in the brush thus behaves like an ideal chain subjected to an external potential created by the brush. According to the SCF theory, all statistical properties of the minority chain can be extracted from this potential. Invoking the mean field approximation, the monomer density ρ_{br} and the potential ω satisfy the following SCF equations

$$\begin{aligned}\omega &= \nu\rho_{br} \\ \rho_{br} &= \frac{n_{br}}{Q_{br}} \int_0^N ds q_{br}(\mathbf{r}, s) q_{br}^\dagger(\mathbf{r}, s)\end{aligned}\quad (25)$$

where n_{br} is the total number of brush chains in the system, Q_{br} is the single chain partition function, and q_{br} and q_{br}^\dagger are the end-integrated propagators of the brush chain. The two propagators satisfy the following modified diffusion equation

$$\frac{\partial q}{\partial s} = \frac{1}{6}\nabla^2 q - \omega q \quad (26)$$

where $q \equiv q_{br}$ or q_{br}^\dagger and s is the contour variable of the brush chain. We set the initial condition $q_{br}(\mathbf{r}, 0) = 1$, and $q_{br}^\dagger(\mathbf{r}, 0) = \delta(z - z_0)$ consistent with the requirement that one end of the brush chain is free, while the other end is grafted at $z = z_0$.^{21,23} We use the Dirichlet boundary condition at $z = 0$ and $z = L_z$ representing the impenetrable boundaries. Because the brush is homogeneous along the x and y directions, we restrict our calculation in the region of unit area on the substrate; i.e., we perform a 1-dimensional calculation.

The transition properties are extracted from the end-integrated propagator of the minority chain, i.e., $q_m(z, s)$ and $q_m^\dagger(z, s)$. They are obtained also by solving the modified diffusion equation with the potential $\omega_m \equiv \omega + U_{ads}$ if $s < N_A$,

and $\omega_m \equiv \omega$, if $s > N_A$. The initial conditions are $q_m(z, 0) = 1$, $q_m^\dagger(z, 0) = \delta(z - z_0)$ like for the brush chains. Having determined $q_m(z, s)$ and $q_m^\dagger(z, s)$, one can calculate the free end distribution $P_e(z)$, i.e., the probability to find the N th monomer at position z , via

$$P_e(z) = \frac{q_m^\dagger(z, N)}{\int dz q_m^\dagger(z, N)} \quad (27)$$

The modified diffusion equation is solved in real space by using the Crank–Nicolson scheme.²⁴ The SCF equations are solved iteratively by updating the potential ω with the simple mixing scheme $\omega^{(n+1)} = \omega^{(n)} + \lambda(\nu\rho_{br}^{(n)} - \omega^{(n)})$, where n is the iteration step and λ is a small number controlling the stability of iteration and the speed of convergence. We always take $\lambda = 0.1$ here. The iteration process stops if the iteration error is smaller than 10^{-8} .

MC Simulations

The MC model and method has already been described in detail in our earlier work.⁹ For the convenience of the reader we describe briefly the basic ideal of the MC scheme in the following and refer to ref 9 for details. The MC scheme we adopted here is a coarse-grained off-lattice model and can be viewed as the discretized counterpart of the SCF theory in 3-dimensional space, as SCF theory and MC scheme share the same Hamiltonian.^{25–29} In the MC scheme, the system is discretized into cubic cells with volume a^3 , and the local density is evaluated in each cell by counting the total number of monomers in it divided by the cell volume. The adsorption potential has the same form as that in the SCF theory, i.e., a steplike function with magnitude ε and width the unit length a . We note that the finite discretization in MC renormalizes the excluded volume parameter.⁹ We set the excluded volume parameter ν_{MC} in the MC simulation as $\nu_{MC} = 1$ to model good solvent conditions. To compensate for fluctuation effects and finite grid size effects and obtain better agreement between simulations and SCF calculations, we use $\nu = 0.776$ in the SCF calculations. Figure 10 shows the density profile for monodisperse brushes for $N_{br} = 100$ with several chosen grafting densities. It can be seen that the density profiles are approximately parabolic consistent to theoretical predictions for the strong stretching limit.^{30–33} The density curves obtained from MC are similar to those obtained with the SCF method except that the tail at the brush surface is sharper. This should be responsible to the difference observed in transition behavior.

■ AUTHOR INFORMATION

Corresponding Author

Shuanhu Qi – Key Laboratory of Bio-inspired Smart Interfacial Science and Technology of Ministry of Education, School of Chemistry, Beihang University, Beijing 100191, China; orcid.org/0000-0002-4260-4641; Email: qishuanhu@buaa.edu.cn

Authors

Leonid I. Klushin – Department of Physics, American University of Beirut, Beirut 1107 2020, Lebanon; Institute for Macromolecular Compounds RAS, 1199004 St. Petersburg, Russia
Alexander M. Skvortsov – Chemical-Pharmaceutical University, 197022 St. Petersburg, Russia

Friederike Schmid – Institut für Physik, Johannes Gutenberg-Universität Mainz, D-55099 Mainz, Germany; orcid.org/0000-0002-5536-6718

Complete contact information is available at:
<https://pubs.acs.org/10.1021/acs.macromol.0c00674>

Notes

The authors declare no competing financial interest.

ACKNOWLEDGMENTS

Financial support by the National Natural Science Foundation of China (NSFC) through Grant 21873010 and by the Deutsche Forschungsgemeinschaft (DFG) through Grant Schm 985/13-2, NNIO-a 17-53-12013, and SFB TRR 146 (project C1) is gratefully acknowledged. Simulations have been performed on the computer cluster at Beihang University.

REFERENCES

- (1) Cohen Stuart, M.; Huck, W.; Genzer, J.; Müller, M.; Ober, C.; Stamm, M.; Sukhorukov, G. B.; Szleifer, I.; Tsukruk, V. V.; Urban, M.; Winnik, F.; Zauscher, S.; Luzinov, I.; Minko, S. Emerging applications of stimuli-responsive polymer materials. *Nat. Mater.* **2010**, *9*, 101–113.
- (2) Kocak, G.; Tuncer, C.; Butun, V. pH-responsive polymers. *Polym. Chem.* **2017**, *8*, 144–176.
- (3) Manouras, T.; Vamvakaki, M. Field responsive materials: photo-, electro-, magnetic- and ultrasound-sensitive polymers. *Polym. Chem.* **2017**, *8*, 74–96.
- (4) Wei, M.; Gao, Y.; Li, X.; Serpe, M. J. Stimuli-responsive polymers and their applications. *Polym. Chem.* **2017**, *8*, 127–143.
- (5) Akkiliç, N.; Leermakers, F. A. M.; de Vos, W. M. Responsive polymer brushes for controlled nanoparticle exposure. *Nanoscale* **2015**, *7*, 17871–17878.
- (6) Motornov, M.; Minko, S.; Eichhorn, K.-J.; Nitschke, M.; Simon, F.; Stamm, M. Reversible tuning of wetting behavior of polymer surface with responsive polymer brushes. *Langmuir* **2003**, *19*, 8077–8085.
- (7) Draper, J.; Luzinov, I.; Minko, S.; Tokarev, I.; Stamm, M. Mixed polymer brushes by sequential polymer addition: anchoring layer effect. *Langmuir* **2004**, *20*, 4064–4075.
- (8) Klushin, L. I.; Skvortsov, A. M.; Polotsky, A. A.; Qi, S.; Schmid, F. Sharp and fast: sensors and switches based on polymer brushes with adsorption-active minority chains. *Phys. Rev. Lett.* **2014**, *113*, No. 068303.
- (9) Qi, S.; Klushin, L. I.; Skvortsov, A. M.; Polotsky, A. A.; Schmid, F. Stimuli-responsive brushes with active minority components: Monte Carlo study and analytical theory. *Macromolecules* **2015**, *48*, 3775–3787.
- (10) Lépine, Y.; Caillé, A. The configuration of a polymer chain interacting with a plane interface. *Can. J. Phys.* **1978**, *56*, 403–408.
- (11) Zhang, S.; Qi, S.; Klushin, L. I.; Skvortsov, A. M.; Yan, D.; Schmid, F. Anomalous critical slowdown at a first order phase transition in single polymer chains. *J. Chem. Phys.* **2017**, *147*, No. 064902.
- (12) Zhang, S.; Qi, S.; Klushin, L. I.; Skvortsov, A. M.; Yan, D.; Schmid, F. Phase transitions in single macromolecules: Loop-stretch transition versus loop adsorption transition in end-grafted polymer chains. *J. Chem. Phys.* **2018**, *148*, No. 044903.
- (13) Skvortsov, A. M.; Klushin, L. I.; Gorbunov, A. A. Long and short chains in a polymer brush: a conformational transition. *Macromolecules* **1997**, *30*, 1818–1827.
- (14) Skvortsov, A. M.; Gorbunov, A. A.; Leermakers, F. A. M.; Fleer, G. J. Long minority chains in polymer brush: a first-order adsorption transition. *Macromolecules* **1999**, *32*, 2004–2015.
- (15) Merlitz, H.; He, G.-L.; Wu, C.-X.; Sommer, J.-U. Nanoscale brushes: how to build a smart surface coating. *Phys. Rev. Lett.* **2009**, *102*, 115702.
- (16) Romeis, D.; Sommer, J.-U. Conformational switching of modified guest chains in polymer brushes. *J. Chem. Phys.* **2013**, *139*, No. 044910.
- (17) Qi, S.; Klushin, L. I.; Skvortsov, A. M.; Liu, L.; Zhou, J.; Schmid, F. Tuning transition properties of stimuli-responsive brushes by polydispersity. *Adv. Funct. Mater.* **2018**, *28*, 1800745.
- (18) Zhulina, E. B.; Borisov, O. V.; Priamitsyn, V. A. Theory of steric stabilization of colloid dispersions by grafted polymers. *J. Colloid Interface Sci.* **1990**, *137*, 495–511.
- (19) Edwards, S. F. The statistical mechanics of polymers with excluded volume. *Proc. Phys. Soc., London* **1965**, *85*, 613–624.
- (20) Helfand, E. Theory of inhomogeneous polymers: fundamentals of the Gaussian random-walk model. *J. Chem. Phys.* **1975**, *62*, 999.
- (21) Fredrickson, G. H. *The Equilibrium Theory of Inhomogeneous Polymers*; Oxford University Press: Oxford, 2006.
- (22) Schmid, F. Self-consistent field theories for complex fluids. *J. Phys.: Condens. Matter* **1998**, *10*, 8105–8138.
- (23) Müller, M. Phase diagram of a mixed polymer brush. *Phys. Rev. E: Stat. Phys., Plasmas, Fluids, Relat. Interdiscip. Top.* **2002**, *65*, No. 030802.
- (24) Drolet, F.; Fredrickson, G. H. Combinatorial screening of complex block copolymer assembly with self-consistent field theory. *Phys. Rev. Lett.* **1999**, *83*, 4317–4320.
- (25) Laradji, M.; Guo, H.; Zuckermann, M. J. Off-lattice Monte Carlo simulation of polymer brushes in good solvents. *Phys. Rev. E: Stat. Phys., Plasmas, Fluids, Relat. Interdiscip. Top.* **1994**, *49*, 3199–3206.
- (26) Besold, G.; Guo, H.; Zuckermann, M. J. Off-lattice Monte Carlo simulation of the discrete Edwards model. *J. Polym. Sci., Part B: Polym. Phys.* **2000**, *38*, 1053–1068.
- (27) Detcheverry, F. A.; Kang, H.; Daoulas, K. C.; Muller, M.; Nealey, P. F.; de Pablo, J. J. Monte Carlo simulations of a coarse grain model for block copolymers and nanocomposites. *Macromolecules* **2008**, *41*, 4989–5001.
- (28) Qi, S.; Behringer, H.; Schmid, F. Using field theory to construct hybrid particle–continuum simulation schemes with adaptive resolution for soft matter systems. *New J. Phys.* **2013**, *15*, 125009.
- (29) Frenkel, D.; Smit, B. *Understanding Molecular Simulation: From Algorithms to Applications*; Academic Press: New York, 2002.
- (30) Milner, S. T.; Witten, T. A.; Cates, M. E. Theory of the grafted polymer brush. *Macromolecules* **1988**, *21*, 2610–2619.
- (31) Zhulina, E. B.; Priamitsyn, V. A.; Borisov, O. V. Structure and conformational transitions in grafted polymer chain layers: a new theory. *Polym. Sci. U. S. S. R.* **1989**, *31*, 205–216.
- (32) Zhulina, E. B.; Borisov, O. V.; Priamitsyn, V. A. Theory of steric stabilization of colloid dispersions by grafted polymers. *J. Colloid Interface Sci.* **1990**, *137*, 495–511.
- (33) Halperin, A.; Kröger, M.; Zhulina, E. B. Colloid-brush interactions: the effect of solvent quantities. *Macromolecules* **2011**, *44*, 3622–3638.
- (34) Paul, W.; Baschnagel, J. *Stochastic Processes: From Physics to Finance*; Springer: Berlin, 1999.
- (35) de Gennes, P.-G. Some conformation problems for long macromolecules. *Rep. Prog. Phys.* **1969**, *32*, 187–205.
- (36) Grassberger, P. J. Simulations of grafted polymers in a good solvent. *J. Phys. A: Math. Gen.* **2005**, *38*, 323–331.
- (37) Klushin, L. I.; Polotsky, A. A.; Hsu, H.-P.; Markelov, D. A.; Binder, K.; Skvortsov, A. M. Adsorption of a single polymer chain on a surface: Effects of the potential range. *Phys. Rev. E* **2013**, *87*, No. 022604.
- (38) Challa, M.; Landau, D.; Binder, K. Monte Carlo studies of finite-size effects at first-order transitions. *Phase Transitions* **1990**, *24*–26, 343–369.